Physics Letters B 811 (2020) 135859

Contents lists available at ScienceDirect

Physics Letters B

www.elsevier.com/locate/physletb

Tachyon field in loop cosmology

Kui Xiao

Department of Science of Mathematics and Physics and Technology of Energy, Hunan Institute of Technology, Hengyang 421002, China

ARTICLE INFO

Article history:
Received 24 March 2020
Received in revised form 8 October 2020
Accepted 9 October 2020
Available online 15 October 2020
Editor: M. Trodden

Keywords:
Modified loop cosmology
Tachyon field
Inflation theory

ABSTRACT

The evolutionary pictures of tachyon field in modified loop cosmology have been investigated. We present the dynamical behavior of the tachyon field associated with an exponential potential and find that the pre-inflation dynamics are very similar in both modified loop cosmology and standard loop quantum cosmology. In addition, tachyonic inflation in modified loop cosmology models are discussed, and we find that the probability of inflation in modified loop cosmology is very closer to 1.

1. Introduction

In the framework of general relativity, both big-bang and black-hole singularities appear that pose some difficulties. To solve the problems associated with these singularities, one possible solution is modifying the theory of general relativity at the high-energy scale. Loop quantum gravity (LQG) is one of the main candidates of these theories [1–3]. Loop quantum cosmology (LQC) is a canonical quantization of homogeneous spacetimes based upon the techniques used in LQG [4–7]. In the past twenty years, many meaningful conclusions have been drawn on solving the singularities of the big bang and black holes within the LQC context [8]. In this scenario, many interesting results have been obtained, e.g., the replacement of the big bang by a big bounce [9–11], the avoidance of most singularities [12–20], and the more likely occurrence of inflation [21–28].

Although LQC has achieved much in inflation theory and singularity theory of the big bang, the relationship between LQC and LQG nevertheless remains to be further explored [29,30]. In this regard, how the various quantization ambiguities affect physical predictions needs to be investigated. Because of ambiguities in the quantization process, different effective Hamiltonians can result in a homogeneous spacetime in loop cosmology [31]. Yang and colleagues obtained two different effective Hamiltonians and found two variants of LQC [32]. Following Ref. [31], these two different LQC models are labeled as mLQC-I and mLQC-II, respectively. In the mLQC-I scenario, the extrinsic curvature in the Lorentzian term is directly described in term of holonomies, whereas in mLQC-II, the proportionality between the extrinsic curvature and the Ashtekar–Barbero connection is used before expressing it in terms of holonomies [31]. Recently, details of these two modified theories have been investigated in many studies [31,33–41]. Similar to the results in LQC, the big-bang singularity is replaced by a quantum bounce, and slow-roll inflation is an attractor in the modified loop cosmology [31,39]. Using a field described by chaotic and Starobinsky potentials and taking into account the kinetic energy dominating (KED) the field at the bounce, the evolution of the Universe can be divided into three different phases: bouncing, damping, and slow-roll inflation [39]. Moreover, the probability that the desired slow-roll inflation does not occur in LQC is smaller than the result for mLQC-I and larger than the one for mLQC-II [39].

In this work, we investigate the tachyonic inflation in modified loop cosmology. We discuss the evolution pictures of the field in Sec. 2 and investigate the tachyonic inflation theory in Sec. 3. To compare the differences in evolutionary behavior of the tachyon field in modified loop cosmology and LQC, all the calculations are based on modified loop cosmology and the LQC scenario in Sec. 2 and 3. In the last section, we present a short conclusion. In this work, we set $G = \hbar = c = 1$.

2. Evolution of the field in modified loop cosmology

We first provide an overview of the modified Friedmann dynamics for mLQC-II, mLQC-I, and LQC and then discuss the evolutionary pictures for the background field. For a detailed discussion of these models, we refer the reader to [10,31,35]. We focus on a spatially flat Friedmann–Robertson–Walker Universe.

E-mail address: 87xiaokui@gmail.com.

https://doi.org/10.1016/j.physletb.2020.135859

2.1. mLQC-II

The effective dynamics of mLQC-II is discussed in Ref. [31]. Here, we briefly introduce the main results of [31]. The Hamiltonian for mLQC-II reads

$$\begin{aligned}\mathcal{H}^{\mathrm{II}} &= \mathcal{H}^{\mathrm{II}}_{\mathrm{grav}} + \mathcal{H}_M \\ &= -\frac{3v}{2\pi\lambda^2\gamma^2}\sin^2\left(\frac{\lambda b}{2}\right)\left[1+\gamma^2\sin^2\left(\frac{\lambda b}{2}\right)\right] + \mathcal{H}_M, \end{aligned} \tag{1}$$

in which $\mathcal{H}_M$ denotes the Hamiltonian of matter, $v \equiv v_0 a^3$, v_0 being the volume of a fiducial cell in the $\mathbb{R}^3$ spatial manifold, a denotes the scale factor, and $b \equiv \gamma H$ in the classical limit, where $H \equiv \dot{a}/a$ gives the Hubble rate and γ denotes the Barbero–Immirzi parameter which is set to $\gamma \approx 0.2375$ [42]. The dot denotes derivative with respect to cosmic time. The variables v and b satisfy the canonical relation $\{b, v\} = 4\pi\gamma$, and parameter λ is defined as $\lambda \equiv \sqrt{4\sqrt{3}\pi\gamma\ell_{Pl}^2}$. This effective Hamiltonian (1) yields the Hamilton's equations

$$\dot{v} = \frac{3v\sin(\lambda b)}{\gamma\lambda}\left[1+\gamma^2-\gamma^2\cos(\lambda b)\right], \tag{2}$$

$$\dot{b} = -\frac{6\sin^2(\lambda b/2)}{\gamma\lambda^2}\left[1+\gamma^2\sin^2\left(\frac{\lambda b}{2}\right)\right] - 4\pi\gamma P, \tag{3}$$

in which $P \equiv -\partial\mathcal{H}_M/\partial v$ denotes the pressure of the field.

The modified Friedmann equation in mLQC-II [31] is

$$\begin{aligned}H^2 &= \frac{16\pi\rho}{3}\left(1-\frac{\rho}{\rho_c^{\mathrm{II}}}\right) \\ &\times \left[\frac{1+4\gamma^2(1+\gamma^2)\rho/\rho_c^{\mathrm{II}}}{1+2\gamma^2\rho/\rho_c^{\mathrm{II}}+\sqrt{1+4\gamma^2(1+\gamma^2)\rho/\rho_c^{\mathrm{II}}}}\right], \end{aligned} \tag{4}$$

in which $\rho_c^{\mathrm{II}} = 4(1+\gamma^2)\rho_c$ with critical energy density $\rho_c = 3/(8\pi\gamma^2\lambda^2)$ in LQC.

2.2. mLQC-I

The effective Hamiltonian and the modified Planck scale dynamics for mLQC-I is introduced in [35]. The effective Hamiltonian for mLQC-I reads

$$\begin{aligned}\mathcal{H}^{\mathrm{I}} &= \mathcal{H}^{\mathrm{I}}_{\mathrm{grav}} + \mathcal{H}_M \\ &= \frac{3v}{8\pi\lambda^2}\left[\sin^2(\lambda b) - \frac{(1+\gamma^2)\sin^2(2\lambda b)}{4\gamma^2}\right] + \mathcal{H}_M. \end{aligned} \tag{5}$$

Hamilton's equations for v and b are

$$\dot{v} = \frac{3v\sin(2\lambda b)}{2\gamma\lambda}\left[(1+\gamma^2)\cos(2\lambda b) - \gamma^2\right], \tag{6}$$

$$\dot{b} = \frac{3\sin^2(\lambda b)}{2\gamma\lambda^2}\left[\gamma^2\sin^2(\lambda b) - \cos^2(\lambda b)\right] - 4\pi\gamma P. \tag{7}$$

Different from mLQC-I and LQC, the Friedmann equation in the contracting phase is different from that in the expanding phase. In the expanding phase, the Friedmann equation reads [35]

$$H^2 = \frac{8\pi\rho}{3}\left(1-\frac{\rho}{\rho_c^{\mathrm{I}}}\right)\left[1+\frac{\gamma^2\rho/\rho_c^{\mathrm{I}}}{(1+\gamma^2)(1+\sqrt{1-\rho/\rho_c^{\mathrm{I}}})^2}\right], \tag{8}$$

in which $\rho_c^{\mathrm{I}} = \rho_c/[4(1+\gamma^2)]$, whereas in the contracting phase,

$$H^2 = \frac{8\pi\alpha\rho_\Lambda}{3}\left(1-\frac{\rho}{\rho_c^{\mathrm{I}}}\right)\left[1+\frac{\rho(1-2\gamma^2+\sqrt{1-\rho/\rho_c^{\mathrm{I}}})}{4\gamma^2\rho_c^{\mathrm{I}}(1+\sqrt{1-\rho/\rho_c^{\mathrm{I}}})}\right], \tag{9}$$

where $\alpha \equiv (1-5\gamma^2)/(1+\gamma^2)$, and $\rho_\Lambda = 3/[8\pi\alpha\lambda^2(1+\gamma^2)^2]$.

2.3. LQC

In the LQC scenario, the effective Hamiltonian is given by [10]

$$\mathcal{H}^{\mathrm{LQC}} = \mathcal{H}^{\mathrm{LQC}}_{\mathrm{grav}} + \mathcal{H}_M = -\frac{3v\sin^2(\lambda b)}{8\pi\gamma^2\lambda^2} + \mathcal{H}_M, \tag{10}$$

from which one obtains

$$\dot{v} = \frac{3v}{2\lambda\gamma}\sin(2\lambda b), \tag{11}$$

$$\dot{b} = -\frac{3\sin^2(\lambda b)}{2\gamma\lambda^2} - 4\pi\gamma P. \tag{12}$$

The modified Friedmann equation in LQC is

$$H^2 = \frac{8\pi}{3}\rho\left(1-\frac{\rho}{\rho_c}\right). \tag{13}$$

Note that, the same modified Friedmann equation is obtained while one considers the reduced phase space quantization in LQC, the only difference is the energy density includes two ingredients, the inflaton and the contribution from dust clock [43]. The detail of reduced phase space quantization, please see [43–46] and references therein.

2.4. Tachyon field

We next consider the tachyon field. Tachyon-field inflation was introduced by Sen [47,48] and also studied in the LQC scenario [49–54] with a Hamiltonian of the field given by

$$\mathcal{H}_m = v\sqrt{V(\phi)^2 + v^{-2}\pi_\phi^2}, \tag{14}$$

in which $V(\phi)$ denotes the potential of the field ϕ, and π_ϕ is the momentum of ϕ, which satisfy

$$\dot{\phi} = \frac{\partial\mathcal{H}_{\mathrm{m}}}{\partial\pi_\phi} = \frac{v\pi_\phi}{\sqrt{V^2+v^{-2}\pi_\phi^2}}, \tag{15}$$

$$\dot{\pi}_\phi = -\frac{\partial\mathcal{H}_{\mathrm{m}}}{\partial\phi} = -\frac{vVV'}{\sqrt{V^2+v^{-2}\pi_\phi^2}}. \tag{16}$$

The energy density and pressure of the tachyon field read

$$\rho = \frac{V}{\sqrt{1-\dot{\phi}}}, \quad P = -V\sqrt{1-\dot{\phi}^2}. \tag{17}$$

It is easy to show that the equation for matter conservation $\dot{\rho} + 3H(\rho+P) = 0$ still holds in modified loop cosmology [31,35]. The equation of motion of the field is

$$\frac{\ddot{\phi}}{1-\dot{\phi}^2} + 3H\dot{\phi} + \frac{V'}{V} = 0, \tag{18}$$

in which prime denotes the derivative with respect to field ϕ. The evolutionary picture for a tachyon with different potentials in the LQC scenario has been discussed in many papers [49–54]. In this work, we focused on the exponential potential

$$V = \beta e^{-\alpha\phi}, \tag{19}$$

with constant parameters α and β; α has dimensions of mass. One always obtains the value of α from observational data, i.e.,

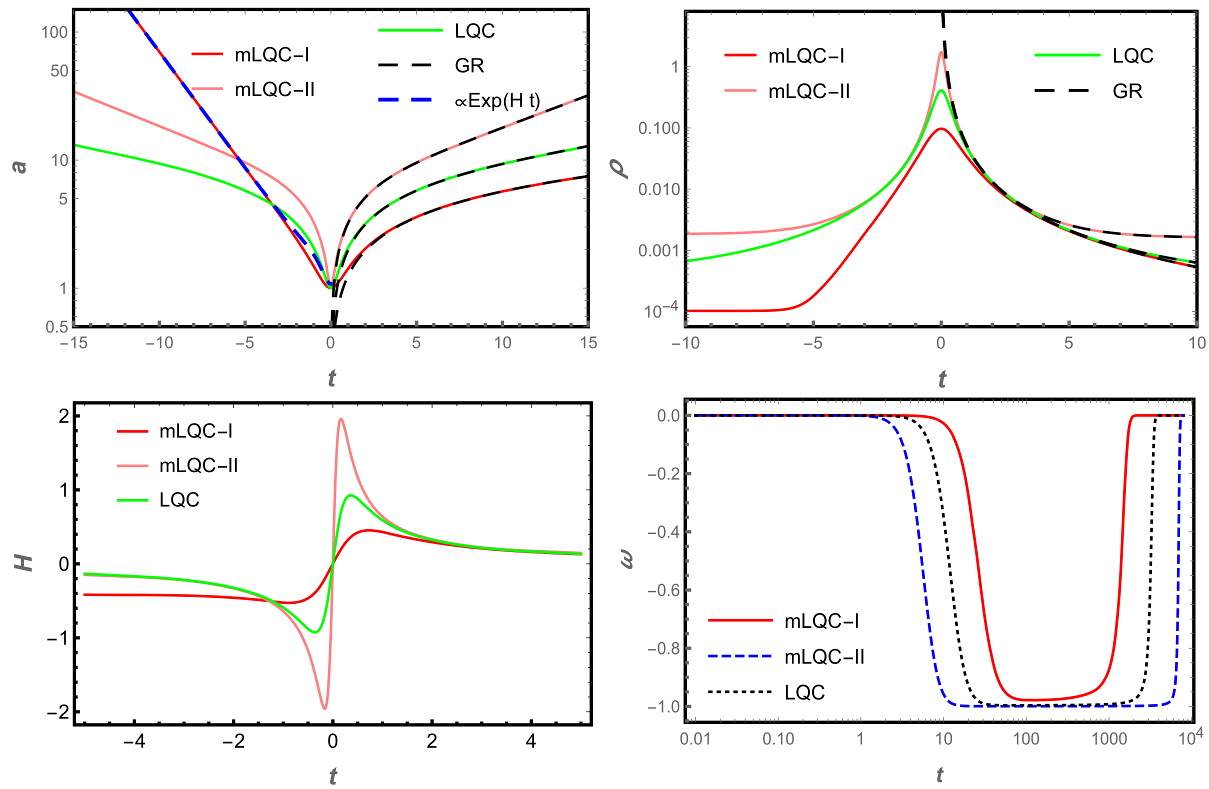

Fig. 1. Comparison of the three models. The initial time is chosen at $t_0 = 10$ and $v_0^{\text{mLQC-I}} = 184.6142$, $v_0^{\text{mLQC-II}} = 5732.9373$, $v_0^{\text{LQC}} = 811.7614$. Three black dashed lines are the results obtained from GR. The blue dashed line is proportional to $e^{H(t)t}$, with the Hubble parameter $H(t)$ of mLQC-I. At the bounce point, $\rho_B/\rho_c^A = 10^{-3}$, $a_B = 1$ for three effective theories, and $\rho_B \to \infty$, $a_B \to 0$ for GR.

the best-fit data from Planck 2018 [55] yielded $\alpha = 5.66 \times 10^{-3}$ [54]. Nevertheless, just as in [50], tachyon-field-sufficient inflation favors a smaller parameter α in the LQC scenario. In this work, we consider $\alpha = 10^{-3}$ and $\beta = \rho_c^A$, with $A = \text{I}, \text{II}$ for mLQC-I and mLQC-II, and $\beta = \rho_c$ for LQC.

Next, we focus on the numerical solutions of the considering models. During the numerical analysis, one should monitore the validity of the Hamiltonian constraint $\mathcal{C} = 16\pi\mathcal{H}^A \approx 0$. Also, the numerical errors should be negligible [35,56]. While the Hamiltonian constraint is satisfied initially, it is satisfied at any other moment, since it is conserved $\dot{\mathcal{C}} \approx 0$ [35]. In this case, we first use the effective Hamiltonian constraint $\mathcal{C} = 16\pi\mathcal{H}^A \approx 0$ to figure out the relationship between trigonometric function terms and v, ϕ, π_ϕ, and then substitute the trigonometric function terms in the Hamilton's equations with v, ϕ, π_ϕ to ensure that the Hamilton constraint conditions are met in the solution process. In this case, we just need to solve equations $\dot{v} = f(v,\phi,\pi_\phi), \dot{\phi} = g(v,\phi,\pi_\phi)$ and $\dot{\pi}_\phi = h(v,\phi,\pi_\phi)$, in which $f(v,\phi,\pi_\phi), g(v,\phi,\pi_\phi), h(v,\phi,\pi_\phi)$ are determined by the Hamilton's equations and the relationship between trigonometric function terms and v, ϕ, π_ϕ for each model. Note that, this method is likely reduced phase space analysis which is generally performed using relational clocks [43–46]. This method is adopted in this work during the numerical analysis, and the numerical errors can be negligible.

To see the differences between the three models. We performed numerical simulations with initial conditions $a_B = 1$, $H_B = 0$, and $V(\phi_B) = 10^{-3}\rho_B$, in which subscript "B" signifies values at the bounce point. The results (Fig. 1) elicit several conclusions:

1. The Hubble parameter $H = 0$ at time $t = 0$, at which the quantum bounce occurs. As for LQC, there is a super-inflation stage in which both the Hubble parameter and scale factor increase. The Universe is asymmetric with respect to the bounce in mLQC-I and is symmetric in mLQC-II and LQC, in clear accordance with the scale factor and energy density. In the contracting phase, the scale factor is proportional to $e^{H(t)t}$ in mLQC-I model, in which $H(t)$ is the Hubble parameter. While $t < -5.6745$, the Hubble parameter is almost a constant, $H \simeq -0.4170$, the Universe enter a exponential expansion phase. Since the quantum geometry effects lead to an emergent cosmological constant (more detail analysis, please see Ref. [35,57]). Identical results were presented in [31], in which the Universe is filled with a scalar field. After the bounce, the Universe enters a GR dominates area very quickly for each interesting model, as shown in the first and second figures in Fig. 1.
2. For the equation of state (EoS),

$$\omega = \frac{P}{\rho} = -1 + \dot{\phi}^2. \tag{20}$$

Here, ω is approximately zero in the super-inflation stage, then decreases to -1, and subsequently increases ultimately to 0 again. The duration for which $\omega = -1$ depends on the model. Moreover, the duration for which $\omega = -1$ in mLQC-II is longest, followed by LQC; mLQC-I yields the shortest duration.

Above, we briefly discussed the evolutionary pictures for modified loop cosmology and found that the EoS enters a stage for which $\omega = -1$ for each model. We next investigate the tachyonic inflation in modified loop cosmology.

3. Inflation theory

As shown in Ref. [54], the probability of a tachyonic inflation in the LQC scenario is very close to 1 for a field with an expo-

Table 1
Quantities involved in the evolution of the background field. The symbol "–" signify that a value does not exist.

	F_B	$t^{\rm SI}_{\rm end}$	$N^{\rm SI}$	$t^{\rm DA}_{\rm end}$	$N^{\rm DA}$	$t^{\rm SL}_{\rm end}$	$N^{\rm SL}$
mLQC-II	10^{-2}	0.1634	0.2224	2.7864	1.7657	2.2597×10^4	4.2237×10^3
	10^{-3}	0.1633	0.2223	9.2118	2.5694	7.0070×10^3	4.0534×10^2
	1.6315×10^{-4}	0.1633	0.2223	25.1710	3.2644	2.7074×10^3	60.0021
	10^{-4}	0.1633	0.2223	33.9579	3.4803	2.0753×10^3	35.0992
mLQC-I	10^{-2}	0.7195	0.2290	0.5383	1.8121	4.7924×10^3	2.1790×10^2
	2.9156×10^{-3}	0.7194	0.2289	25.1398	2.2961	2.7078×10^3	60.0002
	10^{-3}	0.7194	2289	50.3078	2.8112	1.5025×10^3	18.1830
	10^{-4}	0.7194	0.2289	–	–	–	–
LQC	10^{-2}	0.3561	0.2311	5.8625	1.7733	1.0881×10^4	9.7851×10^2
	10^{-3}	0.3564	0.2310	20.2870	2.6227	3.3023×10^3	89.4650
	6.8965×10^{-4}	0.3564	0.2310	25.1769	2.7751	2.7075×10^3	60.0050
	10^{-4}	0.3564	0.2310	–	–	–	–

nential potential and is easier to undergo enough e-foldings while the potential energy dominates at the bounce point. In this work, we consider simply a KED case at the bounce point. To discuss the tachyonic inflation in modified loop cosmology, we first introduce the ratio between $V(\phi_B)$ and ρ_B setting

$$F_B = \frac{V(\phi_B)}{\rho_B}, \tag{21}$$

with $\rho_B = \rho_c^{\rm A}$ for mLQC-I and mLQC-II, and $\rho_B = \rho_c$ for LQC, as mentioned before; then $F_B = e^{-\alpha\phi_B}$. In considering just a KED case, we take $F_B \in (0, 10^{-2}]$. Note that $F_B \neq 0$ because $V(\phi_B) \neq 0$, as given by Eq. (17). For the initial conditions chosen, we obtained interesting numerical results from our models.

For a KED case, three different phases appear between the quantum bounce and re-heating: super-inflation (SI), damping (DA), and slow-roll inflation (SL). We calculated the e-folding number N during these three different phases and is defined as

$$N \equiv \ln\left(\frac{a_{\rm end}}{a_{\rm i}}\right), \tag{22}$$

in which the subscript "i (end)" denotes the value of the scale factor at the start (end) of the specific phase.

We next introduce definitions of the start (end) times for the three different phases. Obviously, for the SI phase, the start time begins at the bounce and ends when $H = H_{\max}$; we denote the variables $\Box$ during this phase as $\Box^{\rm SI}$. For the DA phase, the start time begins at the time that $H = H_{\max}$, and ends when the Hubble parameter $|\varepsilon_H| = 0.1$ for the first time after the bounce. The Hubble parameter is defined as

$$\varepsilon_H = -\frac{\dot{H}}{H^2}. \tag{23}$$

We denote the variables $\Box$ during this phase as $\Box^{\rm DA}$. During the SL phase, the EoS holds its value $\omega = -1$ initially, but increases slightly. We consider the SL phase to end when the EoS increases to $-1/3$ and begins when $|\varepsilon_H| = 0.1$. We denote the variables $\Box$ during this phase by $\Box^{\rm SL}$. Obviously, $t^{\rm SI}_{\rm end} = t^{\rm DA}_{\rm i}$ and $t^{\rm DA}_{\rm end} = t^{\rm SL}_{i}$.

Setting $v_B = 1$ at the bounce point, the initial conditions only depend on the values of F_B. The kinetic energy at the bounce point is a function of F_B, and $\dot{\phi}_B = \sqrt{1 - F_B^2}$. For a KED case, $F_B \in (0, 10^{-2}]$, and hence $\dot{\phi}_B \in (0, 10^{-4}]$. However, just as Table 1 shows, when $F_B < 10^{-4}$, the number of e-foldings is insufficient, and therefore we just consider $F_B \in [10^{-4}, 10^{-2}]$ in this work.

The results of the numerical analysis are presented in Table 1. For each model, the duration of SI phase does not depend on the initial condition, and the e-folding number is almost the same for the all initial conditions considered. This result is the same as for a scalar-field inflation in the LQC scenario [58,59]. Nonetheless, the duration of this phase depends on the model; mLQC-I has the longest duration, LQC the second, and mLQC-II the shortest. For the same initial conditions, the time derivative of H for the mLQC-II scenario is larger than that for LQC and mLQC-I; i.e., $\dot{H}_{\rm B}^{\rm mLQC-II} \simeq 31.3422$, $\dot{H}_{\rm B}^{\rm LQC} \simeq 5.1460$, but $\dot{H}_{\rm B}^{\rm mLQC-I} \simeq 1.2807$.

The duration of the DA phase increases whereas F_B decreases. We consider this phase to start when the Hubble parameter reaches its maximum value. This is different from that for inflation driven by a scalar field in which this phase starts when the kinetic energy equals the potential energy [39]. During this phase, the kinetic energy decreases suddenly, and the Universe soon enters into an accelerating phase. The EoS changes its value rapidly from $\sim -10^{-6}$ to -1 and resembles a step function during this phase (see Fig. 1).

SL phase occurs at time $t^{\rm SL}_{\rm i}$ when $|\varepsilon_H| = 0.1$ for the first time after the bounce, and ends when $\omega = -1/3$ after $t^{\rm SL}_{\rm i}$. During SL phase, the energy is dominated by the potential energy, and $\dot{\phi}^2 \approx 0$; hence, $\omega \simeq -1$. In this work, the assumption that slow roll starts when $|\varepsilon_H| = 0.1$ does not violate the condition $\omega \simeq -1$. For example, $\omega^{\rm A}(t^{\rm SL}_{\rm i}) \leq -0.9326$ for $F_B = 10^{-2}$, and $\omega^{\rm A}(t^{\rm SL}_{\rm i})$ decreases while F_B decrease. In contrast, when SL phase ends, the condition $|\varepsilon_H| < 1$ no longer holds. Indeed, the Hubble parameter $|\varepsilon_H(t^{\rm SL}_{\rm end})| \gtrsim 1$ for all models and all initial conditions considered. Considering the two definitions for the end of SL phase, one being $|\varepsilon_H(t^{\rm SL}_{\rm end})| = 1$ and the other being $\omega(t^{\rm SL}_{\rm end}) = -1/3$, we find that the relative error between the two is always less than 10^{-5}. The duration of SL phase depends on the model and the initial conditions. For all models, choosing a large F_B makes it easier to generate a sufficient number of e-foldings. Under the same conditions, the e-folding number of mLQC-II is larger than that for mLQC-I and LQC. The relative errors between two definitions for the end of SL phase remained similar in Table 1.

From Table 1, one obtains the probability of SL phase for modified loop cosmology. Next, we calculate the probability for tachyonic inflation following [24,39,54]. We first consider the mLQC-II model. The Liouville measure of a phase space Γ with quadruplet variables $(v, b; \phi, \pi_\phi)$ is $d\mu_L = dv db d\phi d\pi_\phi$. The modified Friedmann equation (4) implies that the variables $(v, b; \phi, \pi_\phi)$ must lie on a constraint surface $\bar{\Gamma}$ defined by $\mathcal{H}^{\rm II} \simeq 0$. In contrast, the phase space Γ is isomorphic to a two-dimensional gauge-fixed surface $\hat{\Gamma}$ of $\bar{\Gamma}$ [24,39]. The Liouville measure $d\hat{\mu}$ when pulled back to the surface with constant $b = b_a$ is

$$d\hat{\mu} = \pi_\phi dv d\phi, \tag{24}$$

in which $\pi_\phi = v\sqrt{\frac{9\gamma^4\sin^8\left(\frac{1}{2}\lambda b_a\right)+18\gamma^2\sin^6\left(\frac{1}{2}\lambda b_a\right)+9\sin^4\left(\frac{1}{2}\lambda b_a\right)}{4\pi^2\gamma^4\lambda^4} - V(\phi)^2}$ is a solution of the effective Hamiltonian $\mathcal{C}^{\rm II} = 16\pi\mathcal{H}^{\rm II} \simeq 0$. Obviously, the value of $d\hat{\mu}$ depends on the choice of b_a, which can always be chosen arbitrarily. Nonetheless, there is a preferred value in loop cosmology, specifically, the choice of $b(t)$ at the quantum bounce [24,39], i.e., $\lambda b_a = \lambda b_B$. However, if $\{v(t), \phi(t)\}$ is a solution to Eq. (24), $\{cv(t), \phi(t)\}$ (with constant c) is also a solution. In this case, one can fix $v = v_B = 1$ in the integrals [24]. Then Eq. (24) becomes

$$d\hat{\mu} = \sqrt{\left(\rho_c^{\rm II}\right)^2 - V(\phi)^2} d\phi. \quad (25)$$

Note that, different from Eq. (25) of Ref. [54] in which $d\hat{\mu} \propto \rho_c$, the Liouville measure in mLQC-II is proportional to $\rho_c^{\rm II}$. Therefore, the probability for the desired SL phase is

$$P_{N\geq 60}^{\rm mLQC-II} \simeq \frac{\int_{I(E)} \sqrt{\left(\rho_c^{\rm II}\right)^2 - V(\phi)^2} d\phi}{\int_{\phi_{\min}}^{\phi_{\max}} \sqrt{\left(\rho_c^{\rm II}\right)^2 - V(\phi)^2} d\phi} = \frac{\int_{1.6151\times 10^{-4}}^{1} \sqrt{1 - F_B^2} dF_B}{\int_0^1 \sqrt{1 - F_B^2} dF_B} = 0.999794. \quad (26)$$

In the mLQC-I scenario, following a similar analysis, one obtains probability $P_{N\geq 60}^{\rm mLQC-I} \simeq 0.996288$. For the LQC scenario, according to Eq. (25) of Ref. [54], the probability is $P_{N\geq 60}^{LQC} \simeq 0.999122$. Obviously, $P_{N\geq 60}^{\rm mLQC-II} > P_{N\geq 60}^{\rm LQC} > P_{N\geq 60}^{\rm mLQC-I}$. Therefore, tachyonic inflation is very favorable in modified loop cosmology models. This result is similar to that for an inflation driven by a scalar field with a quadratic potential, in which $P^{\rm mLQC-I}(\text{not realized}) > P^{\rm LQC}(\text{not realized}) > P^{\rm mLQC-II}(\text{not realized})$ [39].

4. Conclusions

In this work, we investigated the evolutionary pictures of tachyon field in modified loop cosmology. We consider two modified loop cosmology, mLQC-I and mLQC-II, and the LQC model has also been discussed. The Universe is asymmetric in mLQC-I unlike the mLQC-II and LQC, which are symmetric with respect to the bounce. The quantum bounce occurs for all considering models when the energy density approaches its maximum value of $\rho_c^{\rm A}$. After the quantum bounce, the Universe enters a SI stage, and then enters a DA phase. The SL happens for a suitable initial condition, during which $\omega = -1$. After the SI phase, the EoS increases to 0 very quickly, and the field acts as cosmic dark matter. The evolutionary images in the cosmology scenario of modified loops are almost similar to those of the LQC scenario.

In the LQC scenario, the probability of obtaining tachyonic inflation with at least 60 e-folds is very close to 1 [54]. In this work, we investigated tachyonic inflation in modified loop cosmology. The duration of each of the three phases depends on the initial conditions and modified model, it being easier to achieve enough e-folds for larger F_B (see Table 1). Moreover, we found that the probability of slow-roll inflation in modified loop cosmology is very close to 1. Note that the probability of tachyonic inflation does not depend on β (see Eq. (26)) but instead depends on α. As argued in Ref. [50], for tachyonic inflation in the LQC scenario, a sufficient inflation favors a smaller α. A smaller α yields a larger probability of a desired slow-roll inflation, i.e., $P^{\rm LQC}(\alpha = 10^{-3}) \simeq 0.999122 > P^{\rm LQC}(\alpha = 5.66 \times 10^{-3}) = 0.999007$. Because the dynamical behaviors of modified loop cosmology and LQC are similar, the same result is easily established, that being, in modified loop cosmology a smaller α gives a larger probability for the desired slow-roll inflation.

Declaration of competing interest

The authors declare that they have no known competing financial interests or personal relationships that could have appeared to influence the work reported in this paper.

Acknowledgements

We thank Dr. Jin-Song Yang and Dr. Cong Zhang for useful discussion. This work is supported by the Education Science Planning Foundation of Hunan Province (Grant No. XJK20BGD049), the Hunan Provincial Natural Science Foundation of China (Grant No. 2017JJ3052), the aid program of the Science and Technology Innovative Research Team of the Hunan Institute of Technology, and the Physics Discipline of the Hunan Institute of Technology. We thank Richard Haase, Ph.D, from Liwen Bianji, Edanz Group China (http://www.liwenbianji.cn/ac), for editing the English text of a draft of this manuscript.

References

[1] C. Rovelli, Quantum Gravity, Cambridge University Press, Cambridge, 2004.
[2] T. Thiemann, Modern Canonical Quantum General Relativity, Cambridge University Press, Cambridge, 2007.
[3] R. Gambini, J. Pullin, A First Course in Loop Quantum Gravity, Oxford University Press, New York, 2011.
[4] M. Bojowald, Loop quantum cosmology, Living Rev. Relativ. 11 (2008) 4.
[5] K. Banerjee, G. Calcagni, M. Martin-Benito, Introduction to loop quantum cosmology, SIGMA 8 (2018) 016.
[6] A. Ashtekar, P. Singh, Loop quantum cosmology: a status report, Class. Quantum Gravity 28 (2011) 213001.
[7] G. Calcagni, Classical and Quantum Cosmology, Springer, Berlin, Germany, 2017.
[8] I. Agullo, P. Singh, Loop quantum cosmology, in: A. Ashtekar, J. Pullin (Eds.), Loop Quantum Gravity: The First 30 Years, World Scientific, 2017.
[9] M. Bojowald, Absence of a singularity in loop quantum cosmology, Phys. Rev. Lett. 86 (2001) 5227.
[10] A. Ashtekar, T. Pawlowski, P. Singh, Quantum nature of the Big Bang: improved dynamics, Phys. Rev. D 74 (2006) 084003.
[11] A. Ashtekar, T. Pawlowshik, P. Singh, Quantum nature of the big bang, Phys. Rev. Lett. 96 (2006) 141301.
[12] P. Singh, A. Toporensky, Big crunch avoidance in k=1 semiclassical loop quantum cosmology, Phys. Rev. D 69 (2004) 104008.
[13] G.V. Vereshchagin, A qualitative approach to semi-classical loop quantum cosmology, J. Cosmol. Astropart. Phys. 0407 (2004) 013.
[14] G. Date, G.M. Hossain, Genericness of a big bounce in isotropic loop quantum cosmology, Phys. Rev. Lett. 94 (2005) 011302.
[15] P. Singh, Are loop quantum cosmos never singular?, Class. Quantum Gravity 26 (2009) 125005.
[16] P. Singh, F. Vidotto, Exotic singularities and spatially curved loop quantum cosmology, Phys. Rev. D 83 (2011) 064027.
[17] P. Singh, Curvature invariants, geodesics, and the strength of singularities in Bianchi-I loop quantum cosmology, Phys. Rev. D 85 (2012) 104011.
[18] K. Bamba, Jaume de Haro, S.D. Odintsov, Future singularities and teleparallelism in loop quantum cosmology, J. Cosmol. Astropart. Phys. 1302 (2013) 008.
[19] A. Joe, P. Singh, Kantowski-Sachs spacetime in loop quantum cosmology: geometric scalars and the viability of quantization prescriptions, Class. Quantum Gravity 32 (2015) 015009.
[20] P. Singh, Loop quantum cosmology and the fate of cosmological singularities, Bull. Astron. Soc. India 42 (2014) 121.
[21] P. Singh, K. Vandersloot, G.V. Vereshchagin, Nonsingular bouncing universes in loop quantum cosmology, Phys. Rev. D 74 (2006) 043510.
[22] A. Corichi, A. Karami, Measure problem in slow roll inflation and loop quantum cosmology, Phys. Rev. D 83 (2011) 104006.
[23] A. Ashtekar, D. Sloan, Loop quantum cosmology and slow roll inflation, Phys. Lett. B 694 (2010) 108.
[24] A. Ashtekar, D. Sloan, Probability of inflation in loop quantum cosmology, Gen. Relativ. Gravit. 43 (2011) 3619.
[25] B. Gupt, P. Singh, A quantum gravitational inflationary scenario in Bianchi-I spacetime, Class. Quantum Gravity 30 (2014) 145013.
[26] L. Linsefors, A. Barrau, Duration of inflation and conditions at the bounce as a prediction of effective isotropic loop quantum cosmology, Phys. Rev. D 97 (2011) 123509.
[27] L. Chen, J.Y. Zhu, Loop quantum cosmology: the horizon problem and the probability of inflation, Phys. Rev. D 92 (2015) 084063.
[28] S. Bedic, G. Vereshchagin, Probability of inflation in loop quantum cosmology, Phys. Rev. D 99 (2019) 043512.

[29] J. Engle, Relating loop quantum cosmology to loop quantum gravity: symmetric sectors and embeddings, Class. Quantum Gravity 24 (23) (2007) 5777.
[30] M. Bojowald, Effective field theory in loop quantum cosmology, Universe 5 (2019) 44.
[31] B.F. Li, P. Singh, A.Z. Wang, Qualitative dynamics and inflationary attractors in loop cosmology, Phys. Rev. D 98 (2018) 066016.
[32] J. Yang, Y. Ding, Y. Ma, Alternative quantization of the Hamiltonian in loop quantum cosmology II: including the Lorentz term, Phys. Lett. B 682 (2009) 1.
[33] M. Assanioussi, A. Dapor, K. Liegener, T. Pawlowski, Emergent de Sitter epoch of the quantum cosmos, Phys. Rev. Lett. 121 (2018) 081303.
[34] Alejandro García-Quismondo, G.A. Mena Marugan, The MMO prescription for the Dapor-Liegener model of loop quantum cosmology, Phys. Rev. D 99 (2019) 083505.
[35] B.F. Li, P. Singh, A.Z. Wang, Towards cosmological dynamics from loop quantum gravity, Phys. Rev. D 97 (2018) 084029.
[36] S. Saini, P. Singh, Generic absence of strong singularities and geodesic completeness in modified loop quantum cosmologies, Class. Quantum Gravity 36 (2019) 105014.
[37] S. Saini, P. Singh, Von Neumann stability of modified loop quantum cosmologies, Class. Quantum Gravity 36 (2019) 105010.
[38] I. Agullo, Primordial power spectrum from the Dapor Liegener model of loop quantum cosmology, Gen. Relativ. Gravit. 50 (2018) 91.
[39] B.F. Li, P. Singh, A.Z. Wang, Genericness of pre-inflationary dynamics and probability of the desired slow-roll inflation in modified loop quantum cosmologies, Phys. Rev. D 100 (2019) 063513.
[40] B.F. Li, P. Singh, A.Z. Wang, Primordial power spectrum from the dressed metric approach in loop cosmologies, arXiv:1912.08225.
[41] S. Saini, P. Singh, Generic absence of strong singularities and geodesic completeness in modified loop quantum cosmologies, Class. Quantum Gravity 36 (2019) 105014, arXiv:1812.08937 [gr-qc].
[42] K.A. Meissner, Black-hole entropy in loop quantum gravity, Class. Quantum Gravity 21 (2004) 5245.
[43] K. Giesel, Bao-Fei Li, P. Singh, Towards a reduced phase space quantization in loop quantum cosmology with an inflationary potential, arXiv:2007.06597 [gr-qc].
[44] K. Giesel, T. Thiemann, Scalar material reference systems and loop quantum gravity, Class. Quantum Gravity 32 (2015) 135015;
K. Giesel, T. Thiemann, Algebraic quantum gravity (AQG). IV. Reduced phase space quantisation of loop quantum gravity, Class. Quantum Gravity 27 (2010) 175009.
[45] K. Giesel, A. Herzog, Gauge invariant canonical cosmological perturbation theory with geometrical clocks in extended phase-space: a review and applications, Int. J. Mod. Phys. D 27 (2018) 183005.
[46] K. Giesel, A. Herzog, P. Singh, Gauge invariant variables for cosmological perturbation theory using geometrical clocks, Class. Quantum Gravity 35 (2018) 155012;
K. Giesel, P. Singh, D. Winnekens, Dynamics of Dirac observables in canonical cosmological perturbation theory, Class. Quantum Gravity 36 (2019) 085009, arXiv:1811.07972.
[47] A. Sen, Tachyon matter, J. High Energy Phys. 07 (2002) 065.
[48] A. Sen, Rolling tachyon, J. High Energy Phys. 04 (2002) 048.
[49] A. Sen, Tachyon field in loop quantum cosmology, Phys. Rev. D 74 (2006) 043501.
[50] H.H. Xiong, J.Y. Zhu, Tachyon field in loop quantum cosmology: inflation and evolution picture, Phys. Rev. D 75 (2007) 084023.
[51] P. Wu, S.N. Zhang, H. Yu, Inverse volume corrections to emergent tachyonic inflation in loop quantum cosmology, J. Cosmol. Astropart. Phys. 05 (2009) 007.
[52] Fei Huang, Jian-Yang Zhu, Kui Xiao, The dynamics of tachyon field with an inverse square potential in loop quantum cosmology, Int. J. Mod. Phys. D 22 (06) (2013) 1350030.
[53] K. Xiao, X.K. He, F. Huang, J.Y. Zhu, Phenomenology analysis of duration inflation for tachyon field in loop quantum cosmology, Int. J. Mod. Phys. D 23 (11) (2014) 1450087.
[54] K. Xiao, Tachyonic inflation in loop quantum cosmology, Eur. Phys. J. C 79 (12) (2019) 1019.
[55] Planck Collaboration, Planck 2018 results. X. Constraints on inflation, arXiv:1807.06211 [astro-ph.CO].
[56] E. Ranken, P. Singh, Nonsingular power-law and assisted inflation in loop quantum cosmology, Phys. Rev. D 85 (2012) 104002.
[57] M. Assanioussi, A. Dapor, K. Liegener, T. Pawłowski, Emergent de Sitter epoch of the Loop Quantum Cosmos: a detailed analysis, Phys. Rev. D 100 (2019) 084003.
[58] T. Zhu, A.Z. Wang, G. Cleaver, Q. Sheng, Universal features of quantum bounce in loop quantum cosmology, Phys. Lett. B 773 (2017) 196.
[59] T. Zhu, A.Z. Wang, G. Cleaver, Pre-inflationary universe in loop quantum cosmology, Phys. Rev. D 96 (2017) 083520.